Biochemical Journal (2019) **476** 1805–1815
https://doi.org/10.1042/BCJ20190143

PORTLAND PRESS

Research Article

Mechanism of nitrite-dependent NO synthesis by human sulfite oxidase

Daniel Bender[1,2], Alexander Tobias Kaczmarek[1,2], Dimitri Niks[3], Russ Hille[3] and Guenter Schwarz[1,2,4]

[1]Department of Chemistry, Institute for Biochemistry, University of Cologne, 50674 Cologne, Germany; [2]Center for Molecular Medicine Cologne, CMMC, University of Cologne, 50931 Cologne, Germany; [3]Department of Biochemistry, University of California, Riverside, CA 92521, U.S.A.; [4]Cologne Cluster of Excellence in Cellular Stress Responses in Aging-associated Diseases, CECAD, University of Cologne, 50931 Cologne, Germany

Correspondence: Guenter Schwarz (gschwarz@uni-koeln.de)

In addition to nitric oxide (NO) synthases, molybdenum-dependent enzymes have been reported to reduce nitrite to produce NO. Here, we report the stoichiometric reduction in nitrite to NO by human sulfite oxidase (SO), a mitochondrial intermembrane space enzyme primarily involved in cysteine catabolism. Kinetic and spectroscopic studies provide evidence for direct nitrite coordination at the molybdenum center followed by an inner shell electron transfer mechanism. In the presence of the physiological electron acceptor cytochrome *c*, we were able to close the catalytic cycle of sulfite-dependent nitrite reduction thus leading to steady-state NO synthesis, a finding that strongly supports a physiological relevance of SO-dependent NO formation. By engineering SO variants with reduced intramolecular electron transfer rate, we were able to increase NO generation efficacy by one order of magnitude, providing a mechanistic tool to tune NO synthesis by SO.

Introduction

In mammals, two biochemical pathways are known for the *de novo* generation of nitric oxide (NO): an oxidative pathway catalyzed by the NO synthases (NOS) [1], and a reductive pathway described as the inorganic nitrate–nitrite–NO pathway [2]. The oxidative pathway utilizes oxygen (O_2) and a guanidine nitrogen derived from arginine to produce citrulline and NO [3]. On the other hand, the reductive nitrate–nitrite-NO pathway is independent of O_2 and is thought to compensate for NO homeostasis at conditions of compromised NOS activity [2]. The reductive pathway requires both nitrate and nitrite *in vivo*, with nitrite being efficiently converted to NO. Both nitrate and nitrite are abundant in the serum and tissue of mammals, although tissue concentrations of nitrite surpass serum concentrations by one order of magnitude [4–6]. Nitrate–nitrite homeostasis is dependent on dietary uptake and the re-oxidation of NO to nitrite and nitrate [7,8].

In the last decades, enzymatic nitrite reduction has been reported for a variety of metal-depending enzymes [9–14]. Among these, all five eukaryotic molybdenum-containing enzymes (i.e. xanthine oxidoreductase, aldehyde oxidase, sulfite oxidase (SO), nitrate reductase and the mitochondrial amidoxime reductase complex, mARC) have been shown to be effective nitrite reductases that generate NO [10,11,13,15,16]. In all these enzymes, nitrite reduction takes place at the molybdenum center, where the metal is complexed in a square-pyramidal manner by a unique tetrahydropyranopterin-based cofactor known as molybdenum cofactor (Moco) [17]. In humans, a defect in Moco biosynthesis leads to loss of activity of all Moco-dependent enzymes resulting in severe neurodegeneration and childhood death [18]. This is mainly attributed to the loss of SO activity, a Moco- and heme-dependent enzyme of the intermembrane space of mitochondria [19], which converts sulfite by oxidation to sulfate as a terminal step in cysteine catabolism. Loss of SO activity leads to accumulation of sulfite and S-sulfonated cysteine, both leading to different forms of cytotoxicity [20].

Received: 26 February 2019
Revised: 21 May 2019
Accepted: 5 June 2019

Accepted Manuscript online: 5 June 2019
Version of Record published: 28 June 2019

PORTLAND PRESS

Biochemical Journal (2019) **476** 1805–1815
https://doi.org/10.1042/BCJ20190143

SO is a homodimer with each subunit divided into three distinct domains [21]. The N-terminal heme domain carries a b_5-type cytochrome linked via a flexible 11-residue tether to the molybdenum-containing domain, where Moco is deeply buried in the protein backbone. The C-terminal dimerization domain promotes homo-dimerization [21]. The two-electron oxidation of sulfite to sulfate occurs at the molybdenum center, which is reduced from Mo^{VI} to Mo^{IV}. Re-oxidation occurs via two intramolecular electron transfers from Mo to heme and from there to the final electron acceptor cytochrome *c*. Both steps depend on protein structural rearrangements enabled by the flexible tether connecting the heme- and molybdenum-containing domains that bring heme transiently into close proximity to the molybdenum center [22]. Following the transfer of a first sulfite-derived electron to heme, the molybdenum center remains reduced by one electron in the Mo^{V} oxidation state [23]. Electron transfer to heme is accompanied by deprotonation of the molybdenum center, resulting in the formation of a hydroxyl moiety bound to Mo^{V}. The Mo^{V} is paramagnetic (with a single d electron) and can be visualized via EPR spectroscopy [24]. Transfer of the electron at heme to cytochrome *c* allows the transfer of the remaining electron in the molybdenum center, leading to completely re-oxidized Mo^{VI} and completion of the catalytic cycle.

We recently reported the reduction in nitrite by SO [11]. We found that the heme domain negatively influenced NO production as illustrated by an SO variant lacking the heme domain, which exhibits enhanced nitrite reduction activity. This suggests a competition between nitrite and heme for sulfite-derived electrons. Interestingly, EPR spectroscopy has shown that sulfite-reduced Mo^{IV} but not Mo^{V} is able to reduce nitrite to NO [11]. In cells, the presence of SO has been shown necessary to promote nitrite-dependent cGMP formation, a proxy for cellular NO levels [11].

In this study, we provide novel insights into the biochemistry of the reduction in nitrite by SO. Using a NO analyzer, we demonstrate stoichiometric conversion of nitrite to NO by sulfite-reduced Mo^{IV} in both full-length SO as well as the molybdenum-containing domain alone. In the presence of the physiological electron acceptor cytochrome *c*, we are able to complete the catalytic cycle showing steady-state NO release. Furthermore, the inert nature of Mo^{V} can be accounted for—on the basis of nitrite reduction—occurring through an inner-sphere electron mechanism at the molybdenum center, which is possible only in the Mo^{IV} oxidation state. Moreover, interfering with heme domain mobility shifts the equilibrium from heme to nitrite reduction within SO, providing a means by which the nitrite-dependent formation of NO can be tuned.

Experimental procedures

Cloning and site-directed mutagenesis of human SO

PCR fragments of human SO cDNA (NM_000456) were cloned into pQE80L (Qiagen, Hilden, Germany) without mitochondrial targeting sequence (Δ1-79; full-length SO) using SacI and SalI as restriction sites and introducing an N-terminal His_6-tag. Heme-deficient SO (SO–Mo) (Δ1-166) was introduced into pQE80L using SacI and HindIII additionally introducing a PreScission protease cleavage site composed of LEVLFQ/GP residues to specifically cleave-off the N-terminal His_6-tag. For site-directed mutagenesis, SO cDNA was used as template and fusion PCR was utilized in order to introduce deletions.

Expression and purification

E. coli TP1004 [25] were transformed with pQE80L-SO constructs. Cells were cultured in 2 l LB medium supplemented with 1 mM sodium molybdate, 100 μg/ml ampicillin, 25 μg/ml kanamycin and grown at 37°C until OD_{600} of 0.6. Expression was induced with the addition of 250 μM IPTG. Cells were grown at 18°C for 72 h and harvested by centrifugation at 5000×***g***. Pellets were re-suspended in buffer containing 50 mM Tris/Ac pH 8.0, 300 mM NaCl and 15 mM imidazole. Cell disruption was achieved by the use of an Emulsiflex-C5 (Avestin) applying a maximum pressure of 2×10^3 psi. Cell debris was pelleted via centrifugation at 20 000×***g*** for 45 min and soluble SO was affinity purified via Ni-NTA gravity flow (Macherey-Nagel). Heme-deficient SO was proteolytically cleaved-off the Ni-NTA matrix by applying 1 mg PreScission protease/ml Ni-NTA matrix in 50 mM Tris/Ac pH 8.0 and 100 mM NaCl *in batch* for 1 h. GST-tagged PreScission protease was removed from the elution by glutathione-affinity purification. Eluted SO was re-buffered in 50 mM Tris/Ac pH 8.0, 30 mM NaCl using PD10 columns (GE Healthcare), frozen in liquid nitrogen and stored at −80°C until further use.

Biochemical Journal (2019) 476 1805–1815
https://doi.org/10.1042/BCJ20190143

Determination of cofactor saturation

The concentration of heme-saturated SO was determined by measuring heme absorption at 413 nm (ε_{413} = 113 000 M^{-1} cm^{-1}). For Moco quantification, 100 pmol SO (based on A_{413}) was used to oxidize Moco to Form-A, which can be quantified by HPLC as described previously [19].

Sulfite-dependent steady-state SO activity

Sulfite-dependent SO activity was determined by either using 50 μM porcine cytochrome *c* (ε_{550} = 19 630 l/mol cm) (BioChemica) or 400 μM ferricyanide ($Fe^{III}(CN)_6$) (ε_{420} = 1020 l/mol cm) as an electron acceptors. Reduction was followed in a time-dependent manner by use of an ELISA reader (EL808 Biotec). The reaction took place in 200 μl 20 mM Bis–Tris/Ac pH 6.5 or 100 mM Tris/Ac pH 8.0 containing SO. The reaction was started with 100 μl sulfite solution of varying concentrations in the appropriate buffer.

Rapid kinetics

Rapid kinetics were performed with an Applied Photophysics Inc.SX-18MV stopped-flow instrument, equipped with a photo diode array detector. Experiments were performed anaerobically at 20°C in 100 mM Tris/Ac pH 8.0. Enzymes and sulfite solutions were prepared anaerobically and mounted on the stopped-flow. Reduction in heme was followed at 423 nm.

NO measurement

NO formation was monitored via a NO analyzer (Model 280i, GE Healthcare) detecting NO by a chemiluminescent reaction with O_3. Via the purge vessel, the NO analyzer was calibrated using defined amounts of sodium nitrite injected in a fully reducing triiodide (I_3^-) solution with argon as carrier gas as described previously [26]. Peak analysis was carried out via Origin software. Nitrite reduction took place in 6 ml 20 mM Bis–Tris/Ac pH 6.5 and 200 or 400 pmol of SO based on Moco concentration. Depending on the experimental setup, sulfite, as well as nitrite concentrations, varied. In the steady-state NO release assay, 5 μM cytochrome *c* was added. Photo-enhanced NO release was achieved by a portable 360 nm UV lamp, which was mounted next to the purge vessel.

Pre-reduction in Moco domain

Heme-deficient SO was pre-reduced anaerobically with 10-fold excess of sulfite (1 mM) in 20 mM Bis–Tris/Ac pH 6.5. The reaction was re-buffered using DextraSEC-PRO2 columns into 20 mM Bis–Tris/Ac pH 6.5. The protein concentration was determined photometrically and 400 pmol of the pre-reduced enzyme was injected into the NO analyzer containing 6 ml 20 mM Bis–Tris pH 6.5, 20 μM sulfite and 2.5 mM nitrite.

Electron paramagnetic resonance spectroscopy

X-band EPR spectra were recorded with the EWWIN 6.0 acquisition and lineshape analysis software (Scientific Software Services) on a Bruker ER 300 spectrometer equipped with an ER035 m gaussmeter and an HP 5352B microwave frequency counter. Temperature was controlled at 150 K using a Bruker ER 4111VT liquid N_2 cryostat. The spectra were acquired by sweeping the magnetic field between 330 and 360 mT. EPR samples were prepared in 20 mM Bis–Tris/Ac pH 6.5 under argon. For EPR spectra of SO, 200 μl 50 μM of the enzyme were incubated in buffer with stirring under an atmosphere of Ar to achieve anaerobicity. Subsequently, 3 μl sulfite and nitrite were added to final concentrations of 300 μM and 20 mM, respectively. Samples were frozen in an ethanol/dry ice bath and EPR spectra were recorded.

Results

Stoichiometric NO release by human SO

Previously, we allocated nitrite reduction to the molybdenum center of SO, where sulfite-reduced Mo^{IV} was shown to reduce nitrite by one electron, while the resulting Mo^{V} was inert to nitrite, suggesting a stoichiometric conversion of nitrite to NO by SO [11]. In order to investigate whether the enzyme produces NO stoichiometrically, full-length human SO was recombinantly expressed and purified (Figure 1A). Based on Moco saturation of the enzyme, 400 pmol full-length SO was injected into the NO analyzer in the presence of 20 μM sulfite and increasing concentrations of nitrite (0.25–5 mM). Traces of enzymatically produced NO (Figure 1B) revealed a peak-like shape, which indicated a single enzymatic turnover rather than a steady-state reaction.

Biochemical Journal (2019) **476** 1805–1815
https://doi.org/10.1042/BCJ20190143

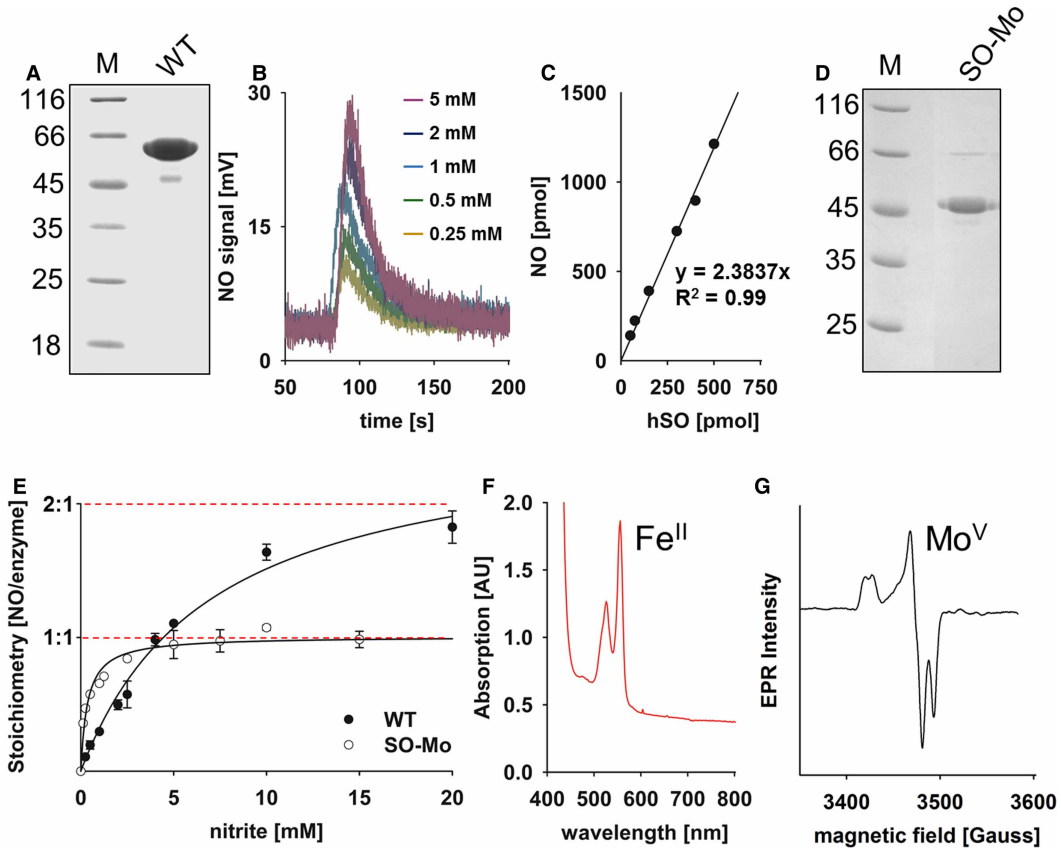

Figure 1. Stoichiometric NO release of full-length and heme-deleted SO.

(**A**) Coomassie-stained 12%-SDS–PAGE of purified full-length human SO. (**B**) NO traces detected by the NO analyzer in 6 ml 20 mM Bis–Tris/Ac pH 6.5, 20 μM sulfite and varying concentrations of nitrite. The reaction was started by injecting 400 pmol of full-length SO. (**C**) SO-dependent NO production at 20 μM sulfite and 20 mM nitrite. (**D**) Coomassie-stained 12%-SDS–PAGE of heme-deleted SO (SO–Mo). (**E**) Nitrite-dependent NO release by full-length SO and SO–Mo. 200 pmol enzyme was injected into 20 μM sulfite and varying concentrations of nitrite. Dashed lines indicate NO/enzyme stoichiometry. (**F**,**G**) Recording of Fe^{II} (UV–vis) and Mo^{V} states (EPR) of full-length SO upon reaction with sulfite and nitrite.

Integration of these peaks allowed the determination of the amount of NO release using a NO calibration curve. The stoichiometry of Moco to NO, produced by the full-length enzyme, was found to be ∼1 : 2 as indicated by plotting the amount of NO formed against the amount of enzyme used under saturating nitrite concentrations (Figure 1C). Based on these results, we concluded that full-length SO released two molecules of NO per monomer.

To investigate whether the 1 : 2 stoichiometry derived from the presence of heme as a second electron acceptor in the full-length enzyme, an N-terminally truncated variant lacking the heme domain (SO–Mo) was recombinantly expressed and purified (Figure 1D). Sulfite- and nitrite-dependent NO formation of SO–Mo revealed a much higher production of NO at low nitrite concentrations (Figure 1E). However, saturation was reached much earlier than with full-length SO leading to a stoichiometry of 1 : 1, which indicated the release of NO and formation of Mo^{V} in a single cycle of sulfite oxidation and nitrite reduction (Figure 1E). These results suggest, that the second NO molecule, which is released by full-length enzyme required the presence of heme, which is able to accept an electron by IET from Mo^{V} following the reduction in one molecule of nitrite by sulfite-reduced SO. The resulting re-oxidized Mo^{VI} is able to react with another sulfite molecule in a second cycle to produce again fully reduced Mo^{IV}, which accepts a second nitrite molecule to produce NO. The resulting Fe^{II}/Mo^{V} intermediate is prohibited from further reaction, thus explaining the 1 : 2 Moco to NO stoichiometry observed in full-length SO.

Biochemical Journal (2019) **476** 1805–1815
https://doi.org/10.1042/BCJ20190143

To verify the Fe^{II}/Mo^{V} state following the 1 : 2 conversion of nitrite to NO by full-length SO, we used UV–vis spectroscopy to detect ferrous iron as well as EPR spectroscopy to detect Mo^{V}. The presence of Fe^{II} was validated by a sharp peak at 555 nm, which is characteristic for reduced b_5-type heme in SO (Figure 1F), confirming the proposed resting state of the enzyme following two cycles of sulfite oxidation and nitrite reduction. EPR spectroscopy revealed the presence of Mo^{V} in the same reaction tube (Figure 1G). In aggregate, these results demonstrate that human SO is able to quantitatively convert nitrite to NO.

Towards the reaction mechanism of nitrite reduction by SO

In the re-oxidation of sulfite-reduced SO, the sulfite-derived electrons are transferred sequentially to the heme, a process that involves the formation of an Mo^{V} intermediate between the two individual electron transfer events (Figure 2A). As we have shown here and in a previous study [11], the Mo^{V} species is inert towards nitrite. In order to elucidate the mechanism of nitrite reduction by Mo^{IV}, SO–Mo was pre-reduced anaerobically with excess sulfite (1 mM) to produce fully reduced Mo^{IV}. Following the reaction, the enzyme was re-buffered to remove the reaction product sulfate and any remaining sulfite. The concentration of the pre-reduced SO–Mo was determined photometrically and the enzyme then injected into the NO analyzer together with 2.5 mM nitrite. In parallel, fully oxidized SO–Mo was injected with 1 mM sulfite and 2.5 mM nitrite together into the NO analyzer. When comparing the amount of released NO, we found that pre-reduction resulted in a significant decrease in detected NO compared with the detected NO, which was produced by an oxidized enzyme following the treatment with sulfite and nitrite simultaneously (Figure 2B,C). Hence, an enzyme in the Mo^{IV} state which is re-oxidized in this way is less prone to reduce nitrite than enzyme that undergoes sulfite oxidation in the presence of nitrite. The likeliest explanation for such a finding suggests an inner-sphere electron transfer mechanism of nitrite reduction as the pre-reduced enzyme presumably co-ordinates H_2O in the equatorial position of molybdenum, which interferes with efficient NO production.

In line with this hypothesis, the previously reported pH dependence of NO formation [11], confirmed here, shows an order of magnitude lower level of NO production at pH 8 than is observed at pH 6.5 (Figure 2D).

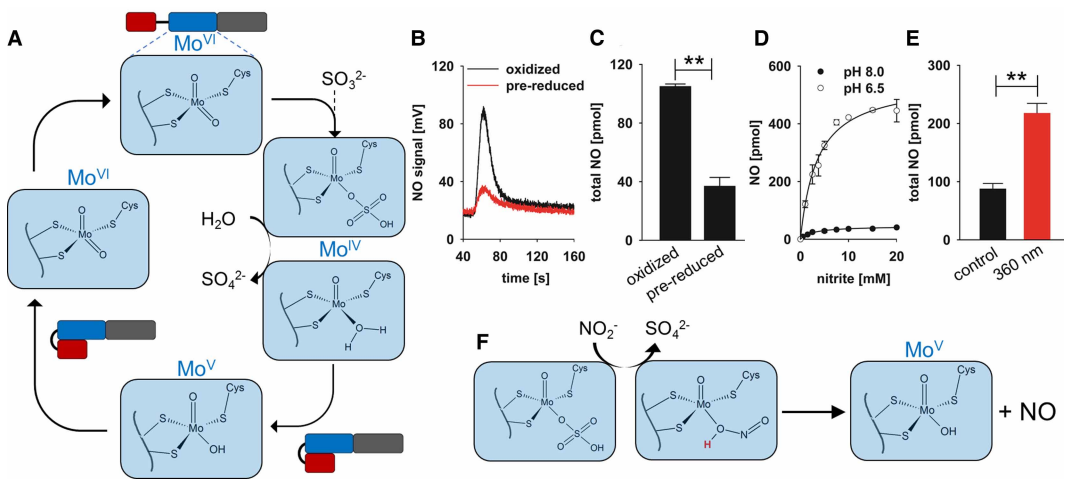

Figure 2. NO release depends on nitrite coordination and protonation.

(**A**) Reaction mechanism of sulfite oxidation by SO. Cartoon of full-length SO monomer shows heme domain (red), Moco domain (blue) and dimerization domain (gray) and the proposed transient interaction of heme and Moco domain upon IET. Light blue boxes indicate Mo coordination sphere in the Moco domain during catalysis. (**B**) Traces of 200 pmol pre-reduced (red) and oxidized (black) SO–Mo injected into the NO analyzer in presence of 2.5 mM nitrite and 20 μM sulfite. (**C**) Quantification of NO released by oxidized and pre-reduced SO–Mo ($n = 3$; $P \leq 0.01$). (**D**) pH dependence of nitrite reduction. 200 pmol full-length enzyme was injected into 20 μM sulfite and varying concentrations of nitrite. 20 mM Tris/Ac or 20 mM Bis–Tris/Ac was used for pH 8.0 and pH 6.5, respectively. (**E**) Quantification of NO amounts released with or without 360 nm irradiation. 200 pmol full-length enzyme injected into 1 mM nitrite and 20 μM sulfite in 6 ml 20 mM Bis–Tris/Ac pH 6.5. (**F**) Proposed nitrite reduction mechanism involving sulfite oxidation, sulfate release and nitrite coordination at Mo with protonation-dependent NO and Mo^{V} release.

Biochemical Journal (2019) **476** 1805–1815
https://doi.org/10.1042/BCJ20190143

This suggests a protonation-sensitive nitrite reduction mechanism. In order to discriminate if nitrite protonation is a prerequisite for NO release or whether the enzyme itself responds to pH differences during nitrite reduction, we used UV-light excitation (360 nm) assuming an accelerated NO release in case of the formation of a proximal Mo-NO_2H bond (Figure 2E). As result, we found a significantly increased NO production following UV-light exposure, consistent with the idea that the SO-catalyzed nitrite reduction requires protonation of a molybdenum-co-ordinated oxygen atom of nitrite as catalytic intermediate towards Mo^V and NO formation (Figure 2F).

Steady-state NO release in the presence of cytochrome *c*

So far only stoichiometric NO release had been shown, which is not expected to be physiologically relevant. In order to demonstrate enzyme-dependent steady-state NO production, a second electron acceptor is necessary to accept the sulfite-derived second electron that otherwise would rest on Mo^V. We therefore added the physiological electron acceptor cytochrome *c* to the reaction mix to determine whether any steady-state NO production was generated. In comparison to a control with inactive SO (Figure 3A) and to a control without cytochrome *c* (Figure 3B), the addition of 10 nmol cytochrome *c* (5 μM) evoked a steady-state NO production by full-length SO that was dependent on the sulfite concentration (Figure 3C). The amount of produced NO was plotted versus the sulfite concentration, which indicated that the highest NO production occurred between 10 and 37.5 μM sulfite, with a dose-dependent inhibition of NO formation at higher sulfite concentrations. At the highest rate, ∼1600 pmol NO was formed with 200 pmol enzyme suggesting eight catalytic cycles per enzyme molecule (Figure 3D).

Sulfite and nitrite both act at the molybdenum center

The requirement of low sulfite concentrations to allow steady-state nitrite reduction in SO suggested that sulfite competes with nitrite, resulting in increased transfer of both sulfite-derived electrons to cytochrome *c*. In order to probe this possibility, the competition of sulfite and nitrite at the molybdenum center of full-length SO was analyzed. First, sulfite-dependent cytochrome *c* reduction was monitored in the absence and presence of 20 mM nitrite (Figure 4A). Nitrite was found to inhibit sulfite-dependent cytochrome *c* reduction at sulfite concentrations ranging from 10 to 100 μM, representing a sulfite concentration range in which steady-state NO production by SO was observed. We also monitored nitrite-dependent NO production in the NO analyzer at two different sulfite concentrations (20 and 100 μM) and found decreased NO production at the higher sulfite concentration (Figure 4B), consistent with competition of sulfite and nitrite at the molybdenum center. Double-reciprocal plots of these data yielded lines intersecting on the *y*-axis, indicative of competitive inhibition of sulfite on NO formation (Figure 4C). Conversely, monitoring NO production in a sulfite-dependent manner at a fixed nitrite concentration showed a reduced NO production at higher sulfite concentrations (Figure 4D).

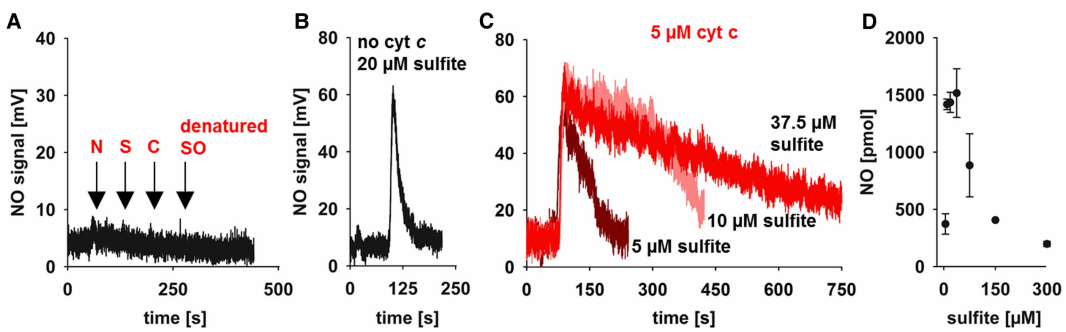

Figure 3. Steady-state NO release of full-length SO in presence of cytochrome *c*.

(**A**) Negative control with no detectable NO release in the NO analyzer upon injection of 20 mM nitrite followed by injection of 20 μM sulfite followed by 5 μM cyt *c* and finally heat-denatured SO boiled at 95°C for 10 min. (**B**) Trace of NO produced by 200 pmol full-length SO at 20 μM sulfite and 20 mM nitrite without cytochrome *c* in 2 ml Bis–Tris/Ac pH 6.5. (**C**) Similar to (**B**) with the addition of 5 μM cytochrome *c* (10 nmol) and increasing sulfite concentrations. (**D**) Sulfite-dependent total NO was calculated by integration of the trace area shown in (**C**) plotted as a function of sulfite concentration. Error bars indicate standard deviation ($n = 3$).

Biochemical Journal (2019) **476** 1805–1815
https://doi.org/10.1042/BCJ20190143

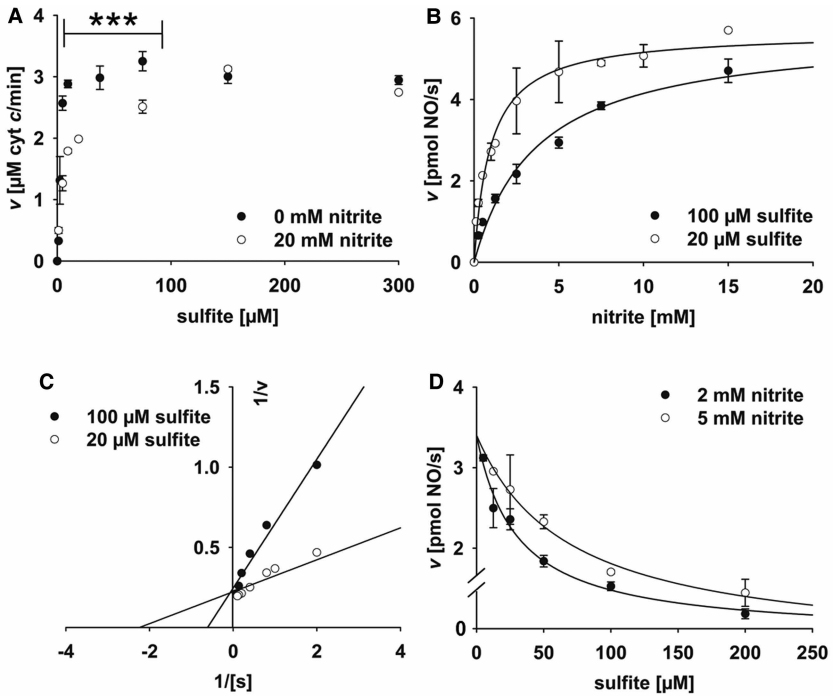

Figure 4. Competition of sulfite and nitrite at the molybdenum center.

(**A**) Sulfite-dependent cytochrome *c* reduction velocities of 10 nM full-length enzyme in the absence (filled circles) and presence (open circles) of 20 mM nitrite. Results are expressed as mean ± standard deviation ($n = 3$; $P \leq 0.001$). (**B**) Nitrite-dependent NO release rate at 20 µM (open circles) and 100 µM sulfite (filled circles) of 200 pmol SO–Mo. (**C**) Lineweaver–Burk diagram of data in (**B**). (**D**) NO rates of 200 pmol SO–Mo at 2 or 5 mM nitrite and varying concentrations of sulfite.

Our results collectively indicate that sulfite and nitrite compete for the molybdenum center and explain the observed decrease in steady-state NO production at higher sulfite concentrations.

Reduction in heme- to Moco domain distance leads to increased nitrite affinity

Since nitrite reduction requires a fully reduced Mo^{IV} center, NO production and electron transfer from Mo^{IV} to the heme compete with each other in full-length SO. It is for this reason that heme domain-deleted SO–Mo exhibited much higher levels of NO production at 100 µM nitrite than did full-length SO enzyme (Figure 5A).

In a previous study, electron transfer within SO was slowed significantly upon truncation of the inter-domain tether by three to five residues [22]. We therefore generated variants in which the tether between heme and Moco domain was truncated even further by 5–11 residues in order to decrease heme mobility and electron transfer (Figure 5B). In total, four truncated SO variants (Δ5, Δ6, Δ8, Δ11) were expressed and purified to homogeneity (Figure 5B) and the impact of tether truncation was analyzed. Using ferricyanide ($Fe^{III}(CN)_6$) as electron acceptor, which acts at the molybdenum center rather than the heme as does cytochrome *c*, all four truncated variants exhibited activities similar to wild-type enzyme (Figure 5C). This indicated that the tether truncation had no effect on sulfite affinity and oxidation at the molybdenum center. The impact of tether truncation on electron transfer from Mo^{IV} to Fe^{III} was analyzed via stopped-flow rapid kinetics. Upon reduction in the molybdenum center by sulfite, subsequent electron transfer to the heme was monitored by the large spectral change in the heme Soret region. All four variants exhibited markedly reduced rates of heme reduction, which slowed as the length of the tether was progressively shortened, from 49.2 ± 6.1 s^{-1} in wild-type SO to 4.1 ± 1.4 s^{-1} in the Δ11 variant having the shortest tether (Figure 5D). The velocity of cytochrome *c* reduction, which depends on heme flexibility and IET rates, was comparably reduced, from 2.5 ± 0.1 µM cytochrome *c*/

Biochemical Journal (2019) **476** 1805–1815
https://doi.org/10.1042/BCJ20190143

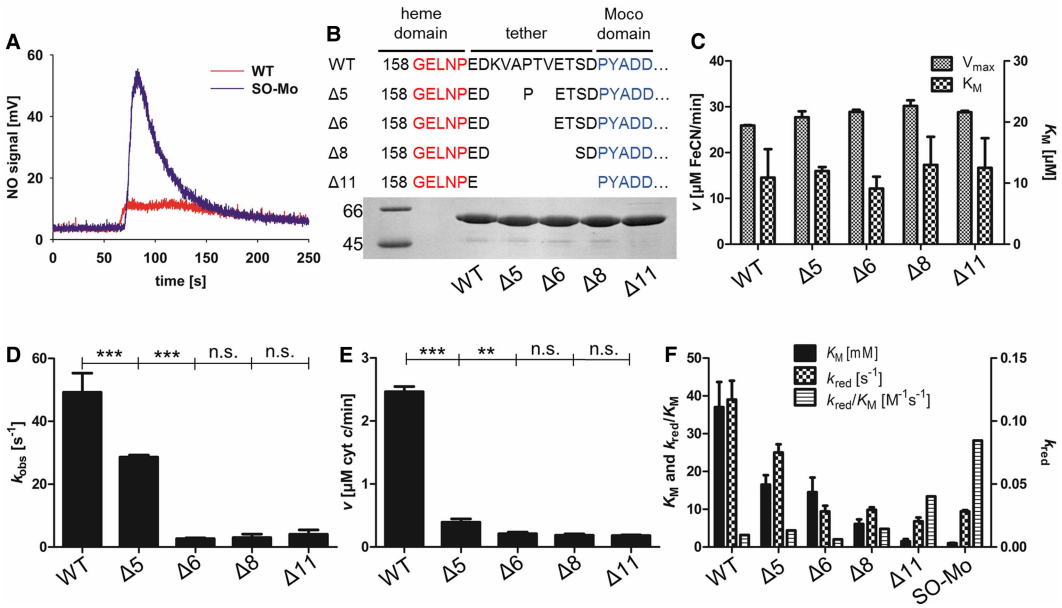

Figure 5. Increased nitrite reduction efficacy by decreasing heme flexibility.

(**A**) NO traces of 2000 pmol full-length SO (red) or heme-deleted SO–Mo (blue) at 100 μM nitrite and 20 μM sulfite. (**B**) Tether region (black) connecting heme- (red) and Moco domain (blue). Tether variants aligned to full-length enzyme. Coomassie brilliant blue staining of purified tether variants after 12% SDS–PAGE. (**C**) Sulfite-dependent FeCN reduction rates of 12.5 nM SO variants and corresponding K_M values ($n = 3$). (**D**) Rapid kinetics of SO variants. 10 μM enzyme was reduced with 500 μM sulfite in 100 mM Tris/Ac pH 8.0. Heme reduction was followed at 423 nm. (**E**) Sulfite-dependent cytochrome *c* reduction in 12.5 nM SO variants at 300 μM sulfite in 100 mM Tris/Ac pH 8.0 ($n = 3$; $P \leq 0.001$ and $P \leq 0.01$). (**F**) Kinetic parameters of SO variants during nitrite reduction. 400 pmol enzyme was injected into the NO analyzer in the presence of 20 μM sulfite and differing concentrations of nitrite.

min for wild-type enzyme to 0.2 ± 0.01 μM cytochrome *c*/min for Δ11 SO (Figure 5E) strongly correlating with the observed changes in internal heme reduction rate.

After demonstrating that progressive tether shortening resulted in ∼10-fold reduction in sulfite-dependent cytochrome *c* reduction velocities with an underlying loss in IET for the Mo^{IV}-heme couple, we next recorded sulfite-dependent nitrite reduction for all SO tether variants (Figure 5F). During stoichiometric NO formation, the height as well as the slope of the NO peak allowed calculation of K_M, k_{red} and k_{red}/K_M values for the individual SO tether variants. We found that the K_M for nitrite decreased gradually with decreasing tether length by more than one order of magnitude from 37.0 ± 6.7 mM nitrite in full-length SO to 1.5 ± 0.6 mM nitrite in Δ11 SO thus closely resembling heme-deleted SO–Mo with a K_M of 1.0 ± 0.1 mM nitrite. In line, the enzymatic efficacy k_{red}/K_M was increased proportionally to tether length ranging from 3.2 M^{-1} s^{-1} in full-length SO to 28.2 M^{-1} s^{-1} in SO–Mo (Figure 5F). In aggregate, our results support the notion that restriction of IET reduces the rate of sulfite-dependent cytochrome *c* reduction, which in turn favors the alternative path of SO catalysis by reducing nitrite to NO.

Discussion

Identification of SO as fourth molybdenum-dependent nitrite reductase in animals underscores the importance of molybdenum-containing enzymes in NO homeostasis [11]. However, the molecular mechanism of nitrite reduction by Moco enzymes remains poorly understood. Here, we investigated nitrite reduction by human SO, demonstrating that nitrite competes with sulfite at the molybdenum center. We provide evidence for a reaction mechanism involving enzyme reduction by sulfite, followed by electron transfer to nitrite and cytochrome *c* followed by re-reduction by sulfite, thus allowing a steady-state catalytic NO formation. Our data are consistent with nitrite coordination to the molybdenum center, presumably at the equatorial position, supporting a computational analysis of nitrite reduction by human mARC, another Moco enzyme [27].

In SO, the one-electron reduction in nitrite to NO by the fully reduced molybdenum center leads to the formation of Mo^V, which cannot reduce a second equivalent of nitrite. With full-length enzyme, however, electron transfer to the heme fully re-oxidizes the molybdenum center, which can then be reduced by a second equivalent of sulfite, generating a second equivalent of NO. The SO–Mo domain alone, however, cannot be re-oxidized and thus produces only a single equivalent of NO. Strikingly, progressive shortening of the polypeptide tether between the molybdenum- and heme-containing domains reduced electron transfer from molybdenum to heme, which in turn allows these variants to generate NO with a much higher efficacy. These findings are in line with previous reports demonstrating domain movement in SO as an important mechanistic feature in the catalytic cycle.

In addition to stoichiometric NO release by SO, we demonstrate steady-state production of NO in the presence of cytochrome *c* with full-length SO. Our finding that this steady-state NO formation is inhibited at increasing sulfite concentrations suggests a competition between sulfite and nitrite for the SO active site. Indeed, we observe nitrite-induced inhibition of sulfite-dependent cytochrome *c* reduction. Strikingly, this inhibition is observed in the same concentration range as that required for steady-state NO synthesis. This indicates that nitrite is an effective alternate electron acceptor in the sulfite-dependent cytochrome *c* reduction, even at elevated concentrations of the physiological electron acceptor [28].

The mechanism for NO production by SO presented here is fully consistent with a computational analysis of nitrite reduction by mARC in which a barrier-less decay of the Mo–nitrite complex to form both Mo^V and NO occurs via a proton-induced disproportionation. The protonation of nitrite, which forms nitrous acid mitigated N–O bonding proximal to the molybdenum, promoting NO release [27]. Nitrite reduction by Fe^{II}-polyoxotungstate complexes occurs in a similar fashion, with proton-dependent NO formation in a first-order manner at or below the pK_A of nitrite [29]. However, the reaction converts to second-order at pH values above the pK_A, which indicates obligate protonation of nitrite as a prerequisite for complex decay and NO release [29].

Similar to the model compound chemistry described above, we find a decline of SO-dependent NO production by one order of magnitude on increasing the pH from 6.5 to 8.0, being consistent with the proton-dependent formation of nitrous acid at a molybdenum-co-ordinated nitrite in the course of NO formation. Interestingly, both nitrite and nitrous acid have absorption maxima between 340 and 370 nm [30]. However, while photolysis of nitrous acid with UV-A light is reported to release a hydroxyl radical and NO in aqueous solution, photolysis of the non-protonated nitrite anion is hampered due to mesomeric stabilization [31,32]. This indicates that proton-dependent nitrous acid formation is a prerequisite for nitrite decay and NO release. Thus, we propose that irradiation-enhanced NO release from SO is dependent on nitrous acid formation at the molybdenum-co-ordinated nitrite. These findings are collectively well in line with pH-dependent nitrite reduction in other metal-centered enzymes [10,13,14,33].

We note that the pH-dependent nitrite reduction in SO is fully compatible with the intracellular localization of the enzyme in the intermembrane space of mitochondria, which is reported to have a pH of 6.8 [34]. Thus, the nitrite reduction capacity of SO at pH 6.5 is reasonably close to the enzyme's physiological environment, which favors proton-dependent nitrite reduction. It might be added that sub-compartmentalization of the mitochondrial intermembrane space itself might lead to local variations in pH [35], which depend on the specific molecular environment. It has been shown that the pH in the vicinity of the proton-pumping complex IV is 0.3 pH units below that at F_0F_1-ATP-synthase [35]. In this respect, the obligate proximity of SO to cytochrome *c* and thus also to complex IV ensures a proton-rich environment. A pH somewhat lower than 6.8 is thus reasonable for the immediate environment of SO. This implies protonation of Mo-co-ordinated nitrite as physiologically more likely than for other mammalian Moco enzymes as well as heme proteins such as hemoglobin, myoglobin and neuroglobin, for which pH sensitivity of nitrite reduction was reported *in vitro* [10,13,14,33].

The physiological significance of SO-derived NO is not yet clear, although the proximity of the enzyme to the respiratory chain raises the possibility of SO being a source of NO to regulate mitochondrial function. It is well known that at least complexes I, III and IV of the respiratory chain are inhibited by NO [36–38], which is considered as a basic mechanism to suppress mitochondria-derived ROS formation. During prolonged ischemia, for example, O_2 restriction prohibits electron flux within the respiratory chain [39] and following tissue re-oxygenation, uncontrolled release of accumulated electrons leads to ROS formation what is commonly referred to as ischemia/reperfusion (IR) injury [40]. ROS formation is, at least in part, controlled by NO-induced inhibition of the respiratory chain, which slows regeneration of respiratory chain activity upon tissue reperfusion [41,42]. In $eNOS^{-/-}$ mice, sensitivity of heart tissue to IR injury increases significantly

Biochemical Journal (2019) **476** 1805–1815
https://doi.org/10.1042/BCJ20190143

compared with control mice. However, the infarct area of these mice is reduced by 50%, when nitrite is added to the drinking water [43]. In humans, nitrite infusion prior to coronary restriction-induced ischemia significantly protects from ROS-induced endothelial dysfunction upon reperfusion [44]. This nitrite-induced preconditioning is attributed to nitrite-derived NO formation, which targets mitochondria and protects cells from IR injury. To date, the enzymatic source(s) for nitrite-derived NO remain a matter of debate. Its proximity to the respiratory chain and the low pH of its surrounding make SO a promising candidate to fulfill a protective role during IR injury and underlines the importance of this enzyme within the nitrate–nitrite–NO pathway.

Abbreviations

IR, ischemia/reperfusion; NO, nitric oxide; NOS, NO synthases; SO, sulfite oxidase; mARC, mitochondrial amidoxime reductase complex.

Author Contribution

D.B. designed and performed experiments, analyzed results and wrote the paper. A.T.K., D.N. and R.H. performed experiments and analyzed results. G.S. designed the study, analyzed results and wrote the paper.

Funding

This work was funded by the Center for molecular medicine Cologne, Germany [Grant number: CMMC2017-C13]. This work was also supported by the US Department of Energy grant DE-SC0010666 (to R.H.).

Acknowledgements

We acknowledge Monika Laurien, Simona Jansen and Joana Stegemann for technical assistance.

Competing Interests

The Authors declare that there are no competing interests associated with the manuscript.

References

1 Knowles, R.G. (1996) Nitric oxide synthases. *Biochem. Soc. Trans.* **24**, 875–878 https://doi.org/10.1042/bst0240875
2 Lundberg, J.O., Weitzberg, E. and Gladwin, M.T. (2008) The nitrate–nitrite–nitric oxide pathway in physiology and therapeutics. *Nat. Rev. Drug Discov.* **7**, 156–167 https://doi.org/10.1038/nrd2466
3 Kwon, S., Nathan, C.F., Gilker, C., Griffith, W. and Stuehr, D.J. (1990) L-citrulline production from L-arginine by macrophage nitric oxide synthase. *J. Biol. Chem.* **265**, 13442–13445 PMID:1696255
4 Kleinbongard, P., Dejam, A., Lauer, T., Rassaf, T., Schindler, A., Picker, O., et al. (2003) Plasma nitrite reflects constitutive nitric oxide synthase activity in mammals. *Free Radic. Biol. Med.* **35**, 790–796 https://doi.org/10.1016/S0891-5849(03)00406-4
5 Bories, P.N. and Bories, C. (1995) Nitrate determination in biological fluids by an enzymatic one-step assay with nitrate reductase. *Clin. Chem.* **41**, 904–907 PMID:7768010
6 Rodriguez, J., Maloney, R.E., Rassaf, T., Bryan, N.S. and Feelisch, M. (2003) Chemical nature of nitric oxide storage forms in rat vascular tissue. *Proc. Natl Acad. Sci. U.S.A.* **100**, 336–341 https://doi.org/10.1073/pnas.0234600100
7 Shiva, S., Wang, X., Ringwood, L.A., Xu, X., Yuditskaya, S., Annavajjhala, V. et al. (2006) Ceruloplasmin is a NO oxidase and nitrite synthase that determines endocrine NO homeostasis. *Nat. Chem. Biol.* **2**, 486–493 https://doi.org/10.1038/nchembio813
8 Joshi, M.S., Ferguson, T.B., Han, T.H., Hyduke, D.R., Liao, J.C., Rassaf, T. et al. (2002) Nitric oxide is consumed, rather than conserved, by reaction with oxyhemoglobin under physiological conditions. *Proc. Natl Acad. Sci. U.S.A.* **99**, 10341–10346 https://doi.org/10.1073/pnas.152149699
9 Cosby, K., Partovi, K.S., Crawford, J.H., Patel, R.P., Reiter, C.D., Martyr, S., et al. (2003) Nitrite reduction to nitric oxide by deoxyhemoglobin vasodilates the human circulation. *Nat. Med.* **9**, 1498–1505 https://doi.org/10.1038/nm954
10 Sparacino-Watkins, C.E., Tejero, J., Sun, B., Gauthier, M.C., Ragireddy, V., Merchant, B.A., et al. (2014) Nitrite reductase and NO synthase activity of the mitochondrial molybdopterin enzymes mARC1 and mARC2. *J. Biol. Chem.* **289**, 10345–10358 https://doi.org/10.1074/jbc.M114.555177
11 Wang, J., Krizowski, S., Fischer-Schrader, K., Niks, D., Tejero, J., Sparacino-Watkins, C., et al. (2015) Sulfite oxidase catalyzes single-electron transfer at molybdenum domain to reduce nitrite to nitric oxide. *Antioxid. Redox Signal.* **23**, 283–294 https://doi.org/10.1089/ars.2013.5397
12 Doel, J.J., Godber, B.L.J., Goult, T.A., Eisenthal, R. and Harrison, R. (2000) Reduction of organic nitrites to nitric oxide catalyzed by xanthine oxidase: possible role in metabolism of nitrovasodilators. *Biochem. Biophys. Res. Commun.* **270**, 880–885 https://doi.org/10.1006/bbrc.2000.2534
13 Li, H., Kundu, T.K. and Zweier, J.L. (2009) Characterization of the magnitude and mechanism of aldehyde oxidase-mediated nitric oxide production from nitrite. *J. Biol. Chem.* **284**, 33850–33858 https://doi.org/10.1074/jbc.M109.019125
14 Tiso, M., Tejero, J., Basu, S., Azarov, I., Wang, X., Simplaceanu, V., et al. (2011) Human neuroglobin functions as a redox-regulated nitrite reductase. *J. Biol. Chem.* **286**, 18277–18289 https://doi.org/10.1074/jbc.M110.159541
15 Zhang, Z., Naughton, D., Winyard, P.G., Benjamin, N., Blake, D.R. and Symons, M.C.R. (1998) Generation of nitric oxide by a nitrite reductase activity of xanthine oxidase: a potential pathway for nitric oxide formation in the absence of nitric oxide synthase activity. *Biochem. Biophys. Res. Commun.* **249**, 767–772 https://doi.org/10.1006/bbrc.1998.9226
16 Dean, J.V. and Harper, J.E. (1988) The conversion of nitrite to nitrogen oxide(s) by the constitutive NAD(P)H-nitrate reductase enzyme from soybean. *Plant Physiol.* **88**, 389–395 https://doi.org/10.1104/pp.88.2.389

17 Schwarz, G., Mendel, R.R. and Ribbe, M.W. (2009) Molybdenum cofactors, enzymes and pathways. *Nature* **460**, 839–847 https://doi.org/10.1038/nature08302
18 Schwarz, G. (2016) Molybdenum cofactor and human disease. *Curr. Opin. Chem. Biol.* **31**, 179–187 https://doi.org/10.1016/j.cbpa.2016.03.016
19 Klein, J. and Schwarz, G. (2012) Cofactor-dependent maturation of mammalian sulfite oxidase links two mitochondrial import pathways. *J. Cell Sci.* **125**, 4876–4885 https://doi.org/10.1242/jcs.110114
20 Kumar, A., Dejanovic, B., Hetsch, F., Semtner, M., Fusca, D., Arjune, S., et al. (2017) S-sulfocysteine/NMDA receptor–dependent signaling underlies neurodegeneration in molybdenum cofactor deficiency. *J. Clin. Invest.* **127**, 4365–4378 https://doi.org/10.1172/JCI89885
21 Kisker, C., Schindelin, H., Pacheco, A., Wehbi, W.A., Garrett, R.M., Rajagopalan, K.V. et al. (1997) Molecular basis of sulfite oxidase deficiency from the structure of sulfite oxidase. *Cell* **91**, 973–983 https://doi.org/10.1016/S0092-8674(00)80488-2
22 Johnson-Winters, K., Nordstrom, A.R., Emesh, S., Astashkin, A.V., Berry, R., Tollin, G. et al. (2010) Effects of interdomain-tether length and flexibility on the kinetics of intramolecular electron transfer in human sulfite oxidase. *Biochemistry* **49**, 1–20 https://doi.org/10.1021/bi901263m
23 Hille, R., Hall, J. and Basu, P. (2014) The mononuclear molybdenum enzymes. *Chem. Rev.* **114**, 3963–4038 https://doi.org/10.1021/cr400443z
24 Rajapakshe, A., Kayunta Johnson-Winters, A.R.N., Meyers, K.T., Emesh, S., Astashkin, A.V. and Enemark, J.H. (2010) Characterization of chloride-depleted human sulfite oxidase by EPR spectroscopy: experimental evidence for the role of anions in product release. *Biochemistry* **49**, 5154–5159 https://doi.org/10.1021/bi902172n
25 Palmer, T., Santini, C.L., Iobbi-Nivol, C., Eaves, D.J., Boxer, D.H. and Giordano, G. (1996) Involvement of the narJ and mob gene products in distinct steps in the biosynthesis of the molybdoenzyme nitrate reductase in *Escherichia coli*. *Mol. Microbiol.* **20**, 875–884 https://doi.org/10.1111/j.1365-2958.1996.tb02525.x
26 MacArthur, P.H., Shiva, S. and Gladwin, M.T. (2007) Measurement of circulating nitrite and S-nitrosothiols by reductive chemiluminescence. *J. Chromatogr. B Anal. Technol. Biomed. Life Sci.* **851**, 93–105 https://doi.org/10.1016/j.jchromb.2006.12.012
27 Yang, J., Giles, L.J., Ruppelt, C., Mendel, R.R., Bittner, F. and Kirk, M.L. (2015) Oxyl and hydroxyl radical transfer in mitochondrial amidoxime reducing component-catalyzed nitrite reduction. *J. Am. Chem. Soc.* **137**, 5276–5279 https://doi.org/10.1021/jacs.5b01112
28 Brody, M.S. and Hille, R. (1999) The kinetic behavior of chicken liver sulfite oxidase. *Biochemistry* **38**, 6668–6677 https://doi.org/10.1021/bi9902539
29 Toth, J.E. and Anson, F.C. (1989) Electrocatalytic reduction of nitrite and nitric oxide to ammonia with iron-substituted polyoxotungstates. *J. Am. Chem. Soc.* **256**, 2444–2451 https://doi.org/10.1021/ja00189a012
30 Reddy Maddigapu, P., Minero, C., Maurino, V., Vione, D., Brigante, M., Charbouillot, T. et al. (2011) Photochemical and photosensitised reactions involving 1-nitronaphthalene and nitrite in aqueous solution. *Photochem. Photobiol. Sci.* **10**, 601–609 https://doi.org/10.1039/c0pp00311e
31 Zellner, R., Exner, M. and Herrmann, H. (1990) Absolute OH quantum yields in the laser photolysis of nitrate, nitrite and dissolved H_2O_2 at 308 and 351 nm in the temperature range 278–353 K. *J. Atmos. Chem.* **10**, 411–425 https://doi.org/10.1007/BF00115783
32 Arakaki, T., Miyake, T., Hirakawa, T. and Sakugawa, H. (1999) Ph dependent photoformation of hydroxyl radical and absorbance of aqueous-phase N(III) ($HNO_2$and NO_2^-). *Environ. Sci. Technol.* **33**, 2561–2565 https://doi.org/10.1021/es980762i
33 Doyle, M.P., Pickering, R.A., DeWeert, T.M., Hoekstra, J.W. and Pater, D. (1981) Kinetics and mechanism of the oxidation of human deoxyhemoglobin by nitrites. *J. Biol. Chem.* **256**, 12393–12398 PMID:7298665
34 Porcelli, A.M., Ghelli, A., Zanna, C., Pinton, P., Rizzuto, R. and Rugolo, M. (2005) pH difference across the outer mitochondrial membrane measured with a green fluorescent protein mutant. *Biochem. Biophys. Res. Commun.* **326**, 799–804 https://doi.org/10.1016/j.bbrc.2004.11.105
35 Rieger, B., Junge, W. and Busch, K.B. (2014) Lateral pH gradient between OXPHOS complex IV and F(0)F(1) ATP-synthase in folded mitochondrial membranes. *Nat. Commun.* **5**, 3103 https://doi.org/10.1038/ncomms4103
36 Clementi, E., Brown, G.C., Feelisch, M. and Moncada, S. (1998) Persistent inhibition of cell respiration by nitric oxide: crucial role of S-nitrosylation of mitochondrial complex I and protective action of glutathione. *Proc. Natl Acad. Sci. U.S.A.* **95**, 7631–7636 https://doi.org/10.1073/pnas.95.13.7631
37 Iglesias, D.E., Bombicino, S.S., Valdez, L.B. and Boveris, A. (2015) Nitric oxide interacts with mitochondrial complex III producing antimycin-like effects. *Free Radic. Biol. Med.* **89**, 602–613 https://doi.org/10.1016/j.freeradbiomed.2015.08.024
38 Sarti, P., Arese, M., Bacchi, A., Barone, M.C., Forte, E., Mastronicola, D. et al. (2003) Nitric oxide and mitochondrial complex IV. *IUBMB Life* **55**, 605–611 https://doi.org/10.1080/15216540310001628726
39 Chen, Q., Moghaddas, S., Hoppel, C.L. and Lesnefsky, E.J. (2008) Ischemic defects in the electron transport chain increase the production of reactive oxygen species from isolated rat heart mitochondria. *Am. J. Physiol. Cell Physiol.* **294**, C460–C466 https://doi.org/10.1152/ajpcell.00211.2007
40 Perrelli, M., Pagliaro, P. and Penna, C. (2011) Ischemia/reperfusion injury and cardioprotective mechanisms: role of mitochondria and reactive oxygen species. *World J. Cardiol.* **3**, 186–200 https://doi.org/10.4330/wjc.v3.i6.186
41 Phillips, L., Toledo, A.H., Lopez-Neblina, F., Anaya-Prado, R. and Toledo-Pereyra, L.H. (2009) Nitric oxide mechanism of protection in ischemia and reperfusion injury. *J. Investig. Surg.* **22**, 46–55 https://doi.org/10.1080/08941930802709470
42 Brown, G.C. (1999) Nitric oxide and mitochondrial respiration. *Biochim. Biophys. Acta, Bioenergetics* **1411**, 351–369 https://doi.org/10.1016/S0005-2728(99)00025-0
43 Bryan, N.S., Calvert, J.W., Gundewar, S. and Lefer, D.J. (2009) Dietary nitrite restores NO homeostasis and is cardioprotective in eNOS deficient mice. *Free Radic. Biol. Med.* **45**, 468–474 https://doi.org/10.1016/j.freeradbiomed.2008.04.040
44 Ingram, T.E., Fraser, A.G., Bleasdale, R.A., Ellins, E.A., Margulescu, A.D., Halcox, J.P. et al. (2013) Low-dose sodium nitrite attenuates myocardial ischemia and vascular ischemia-reperfusion injury in human models. *J. Am. Coll. Cardiol.* **61**, 2534–2541 https://doi.org/10.1016/j.jacc.2013.03.050